Bauhaus-Universität Weimar
20.-22. September 2022
BauSIM2022 in Weimar
ibpsa

AIRFLOW THROUGH A FAÇADE GREENING SYSTEM EQUIPPED WITH VERTICAL PHOTOVOLTAIC MODULES

Theresa Paskert, Hayder Alsaad, Conrad Voelker
Department of Building Physics, Bauhaus-University Weimar
Weimar, Germany
theresa.anna.leonie.paskert@uni-weimar.de, hayder.alsaad@uni-weimar.de, conrad.voelker@uni-weimar.de

Abstract

Using computational fluid dynamics (CFD), this study investigates airflow through a façade greening system equipped with photovoltaic modules. ANSYS Fluent was used to perform steady-state simulations with two-dimensional models. The characteristics of airflow through the vegetation were considered by applying user defined functions (UDF) to the vegetation areas; these UDFs were validated for three k-ε models. The impact of the surroundings roughness was explored using different roughness length values z_0 and using geometrical roughness modeling. Results indicated that compared to an air velocity of about 0.60 m/s at the bare façade, velocities within the greening system varied around 0.15 m/s to 0.50 m/s.

Introduction

The increasing urbanization and related repercussions such as diminishing space for vegetation through densification provoke a complex of problems. An important one is the increasing impact of climate change which leads to phenomena such as the urban heat island effect. The necessity for systems that provide support in coping with the consequences of urbanization and climate change is evident. Façade greening has been often assessed in the literature as a plausible solution to address these issues. The research project VertiKKA (Vertical green water treatment systems for increasing resources efficiency and quality of life in urban areas) suggests a combination of a living wall system (LWS) with integrated decentralized greywater treatment and photovoltaic (PV) modules mounted in front of the foliage (Figure 1). Each of these components has unique benefits. The vegetation can improve air quality as well as reduce the effects of heatwaves (Alsaad et al., 2022a, 2022b). The substrate is designated for greywater treatment, which lowers the sewage load on the city's water treatment centers. Finally, PV modules produce regenerative energy used for operating the system.

While the thermal aspects of greening systems are well documented in the literature, the impact of the greening module on airflow is not fully investigated. The literature shows that airflow is hindered by greening (Perini et al., 2011; Susorova et al., 2014; Gromke et al., 2015). Nevertheless, no concrete statements about airflow and air change rate through the greening system can be found. Since such statement is necessary for hygrothermal assessments of the greening system (Alsaad and Voelker, 2021; Alsaad et al., 2022d, 2022c), the aim of this study is to evaluate the influence of the VertiKKA living wall on airflow by performing steady-state CFD simulations. Before conducting the simulations, the model was first validated using measurement data from the literature.

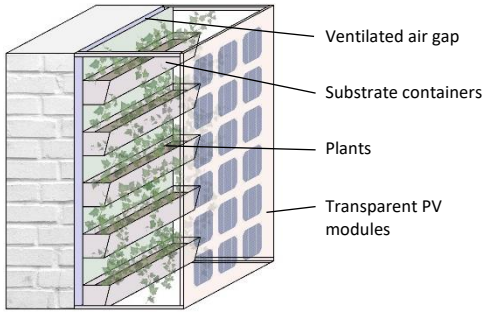

Figure 1: The simulated VertiKKA living wall system

Methodology

Computational domain and numerical settings

The simulations were conducted using a 2D geometry of a building on the campus of the Bauhaus-University Weimar in Weimar, Germany. The geometry included a street canyon with the university building on the outlet side of the domain and the opposite building on the inlet side of the domain. The suggested LWS was mounted on the university building on the first and second floors (Figure 2).

The computational model was created following the best practice guidelines by Franke et al. (2007) and Tominaga et al. (2008). The domain was separated into: (1) outer area with coarse mesh, (2) inner area with medium mesh, (3) a region close to the area of interest with fine mesh, and (4) the area of LWS. The

domain had total dimensions of 438 m x 210 m. These dimensions fulfill the requirement of a maximum vertical blockage ratio BR_H, Eq. (1), which is recommended by Blocken (2015):

$$BR_H = \frac{H_{building}}{H_{domain}} \leq 17\% \quad (1)$$

With $H_{building}$ = 19 m and H_{domain} = 210 m, the blockage ratio equals to 9.05% < 17%. The LWS is shown at the bottom of Figure 2.

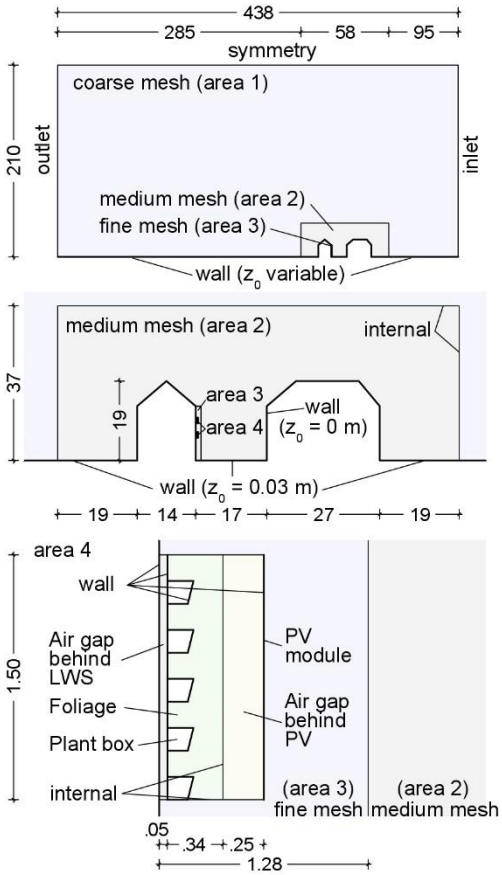

Figure 2: Illustration of the generated domain: full domain (top), closeup of area 2 including areas 3 and 4 (center), area 4 (the LWS) (bottom). Dimensions are in meter

A grid with several sizing regions was defined based on the results of a grid sensitivity study which was conducted to ensure that further refinement of the mesh had no impact on the results. For the grid sensitivity study, an initial grid that fulfilled the requirements of Franke et al. (2007) and Tominaga et al. (2008) was systematically refined. The refinement factor was set to $1.5^n = 2.25$ for a two-dimensional case (n = 2). In this study, five grids were evaluated. Air velocities within the regions of the LWS were compared for each consecutive refinement step, finding a rather fine grid most appropriate. Within the air gap behind the LWS, an edge length of 0.01 m was applied. Within the region of foliage and the area behind PV, the grid was expanded (factor 1.05) from 0.01 m to approximately 0.035 m edge length. The edge length was increased to 0.07 m in area 3. A medium-sized grid with 0.40 m edge length was defined in area 2, expanding to a coarser grid by factor 1.05 within the rest of the domain. This resulted in 45,171 square cells. A logarithmic profile was applied to the inlet boundary using a UDF compiled with following equations for velocity U (Eq. (2)), turbulent kinetic energy k (Eq. (3)), and turbulent dissipation rate ε (Eq. (4)) (Richards and Hoxey, 1993):

$$U(z) = \frac{u_*}{\kappa} \ln\left(\frac{z + z_0}{z_0}\right) \quad (2)$$

$$k(z) = \frac{u_*^2}{\sqrt{c_\mu}} \quad (3)$$

$$\varepsilon(z) = \frac{u_*^3}{\kappa(z + z_0)} \quad (4)$$

where u_* is the friction velocity [m/s], z [m] is the height above the ground with aerodynamic roughness length z_0 [m], κ = 0.42 is the dimensionless van Karman constant, and c_μ = 0.09 [-] is a standard closure constant. The velocity was set to U(z) = 4.2 m/s at z = 10 m according to the Test Reference Year data from the German Meteorological Service. For the ground, the stationary wall boundary condition was chosen with non-slip shear condition. A roughness length of z_0 = 0.03 m was imposed to the ground of area 2. In area 1, the roughness length was increased to z_0 = 0.50 m. The top border was defined as a symmetry boundary condition, and a pressure outlet condition was assigned to the outflow. A wall boundary condition with zero roughness was applied to the walls of the buildings. Corresponding to the work of Gromke and Blocken (2015), a UDF was applied to the foliage area based on the following:

$$S_{U_i} = -\rho C_d LAD U_i \mathbf{U} \quad (5)$$

$$S_k = \rho C_d LAD(\beta_p \mathbf{U}^3 - \beta_d \mathbf{U} k) \quad (6)$$

$$S_\varepsilon = \rho C_d LAD \frac{\varepsilon}{k}(C_{\varepsilon 4}\beta_p \mathbf{U}^3 - C_{\varepsilon 5}\beta_d \mathbf{U} k) \quad (7)$$

Where ρ is the density of air [kg/m³] and C_d = 0.2 [-] is the leaf drag coefficient, LAD is the leaf area density [m²/m³] (set here to 3 m²/m³), U_i [m/s] is the component of velocity of direction i, and U [m/s] is the mean velocity. β_d = 5.1 is a dimensionless coefficient for short-circuiting of the eddy cascade and β_p = 1.0 the fraction of mean flow kinetic energy converted to turbulent kinetic energy. $C_{\varepsilon 4} = C_{\varepsilon 5}$ = 0.9 are dimensionless closure constants. The CFD code ANSYS Fluent was used for solving the RANS equations with the k-ε turbulence model. The choice of the turbulence model is discussed in the validation

section. Heat transfer was not simulated in this study; only the transport and turbulence of the flow. Near-wall treatment was set to standard wall functions. For pressure-velocity coupling, the SIMPLE scheme was used. Spatial discretization was realized with second order upwind for pressure, momentum, turbulent kinetic energy, and turbulent dissipation rate. Test simulations were conducted to determine the sensitivity of the convergence criteria according to Franke et al. (2007). Results of the sensitivity analysis showed that convergence can be assumed when all residuals had fallen below 10^{-6}.

Validation of the vegetation model

The validation for the two-dimensional geometry investigated here was performed based on the work of Gromke and Blocken (2015). Measurement data from Amiro (1990) for an aspen forest was used for validating the CFD results. The simulation was executed for the realizable k-ε (RKE), standard k-ε (SKE) and Re-Normalisation Group k-ε (RNG) model to determine the most appropriate model.

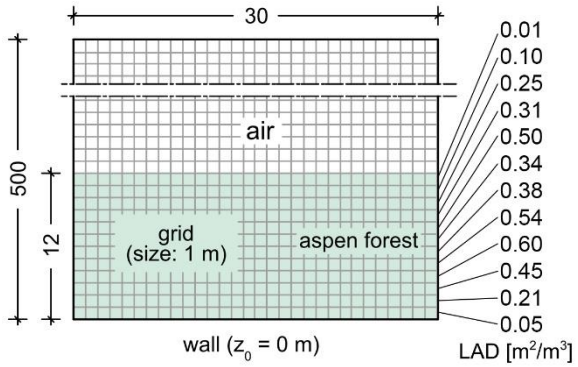

Figure 3: Computational domain of the validation model including the LAD of the aspen forest following the work of Gromke and Blocken (2015)

Computational domain and numerical settings

A two-dimensional geometry with dimensions of L = 30 m and H = 500 m was created. The vegetation was located at the first 12 m of the domain (Figure 3). A mesh of 1 m in size was created and applied throughout the domain resulting in 150,000 square elements. Coupled periodic boundary conditions were applied to the inlet and outlet. The ground was defined as a wall with zero roughness. A symmetry boundary condition was imposed to the top. The UDF representing the airflow through vegetation was applied to the area of foliage. The implemented LAD varied with increasing height according to the measurements of Amiro (1990); the LAD profile is presented on the right side of Figure 3. An air mass flow of 5,000 kg/s was assigned at the inlet corresponding to an air speed at the center of the model of 2.3 m/s at 13.1 m according to the measurement data. Numerical settings for this study are congruent to the previous section, except for the convergence criterion. Once all residuals had fallen below 10^{-4}, convergence was assumed.

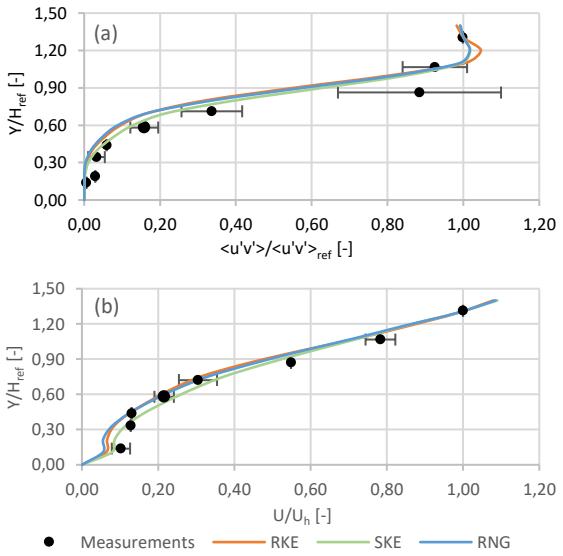

Figure 4: Validation of the normalized kinematic Reynolds stress (a) and normalized stream-wise velocity (b); error bars show standard deviation

Validation results

CFD results for mean stream-wise velocity U and kinematic Reynolds shear stress <u′v′> were regarded on a vertical line in the middle of the domain (X = 15 m). For the comparison of CFD results and measurements, both velocity and shear stress were normalized using the reference velocity U_{ref} and reference Reynolds stress $\langle u'v' \rangle_{ref}$ at 13.1 m height, respectively. Also, the height Y was normalized by H_{ref} = 10 m. Figure 4 (top) shows the simulated Reynolds shear stress compared to the measurements. In general, a good agreement with the measurements and similar attitudes can be seen for all three models with the SKE model yielding the closest results to the measurements. Regarding the results of each model individually, it was noted that for the lower part of the canopy, around $Y/H_{ref} < 0.3$, differences in shear stresses and velocities compared to measurements are relatively high. In this area, absolute quantities are small and therefore large relative differences can occur. For almost all $Y/H_{ref} > 0.3$, the SKE model shows the lowest relative differences with a maximum of 38.6% at $Y/H_{ref} = 0.8$; the other models resulted in even higher relative differences this height. Utilizing the approach of least-squares-method for analyzing quantitative deviations, the squared differences between the measurements and the CFD results are the lowest for the SKE model with 0.132. This is followed by the RNG model with 0.192 and finally the RKE with 0.209. On average, RKE, SKE, and RNG model underestimate the measurement data at around 30%, 17%, and 31%, respectively. Similar tendencies can be found when evaluating the mean wind speed in Figure 4 (bottom). CFD results of the RKE and RNG

models are very alike in characteristics. Velocities from the SKE model are slightly higher compared to the other models. The SKE model reaches its maximum relative difference of 25% at $Y/H_{ref} = 0.4$ and shows high deviation at the other points as well. However, on average, the SKE model deviates the least in comparison to the other two models. The least-squares-method results in differences of 0.0124 for SKE, 0.0192 for RNG, and 0.0204 for RKE model. For RKE and RNG model, velocities on average are underestimated by around 14.5%. Averaging the relative differences for the SKE model results in a slight overestimation of the normalized velocity of less than 1%. In conclusion, the comparisons show that simulations with all three models result in data that is in good agreement with the measurements from Amiro (1990). The SKE model showed the lowest deviation. However, this model led to convergence problems. Therefore, for the simulations discussed in this study, the RKE model was used.

Simulated variations

The first simulated variations consisted of a model with LWS with the settings reported earlier compared to the same model without LWS (bare wall, reference façade). Air velocity through the different areas of the LWS was probed using area weighted averages. The air change rates (ACH) were calculated with $H_{System} = 1.50$ m according to:

$$\mathrm{ACH} = \frac{\mathrm{v}}{\mathrm{H_{System}}} 3600\ \mathrm{s/h} \tag{9}$$

Additionally, to identify the influence of the surroundings on airflow through the LWS, the roughness of the surroundings was systematically varied using two methods: firstly, the roughness length z_0 was varied to 0.10, 0.25, 0.50, and 1.0 m according to classes 4 to 7 of the Davenport-Wieringa roughness classification (Wieringa, 1992). Secondly, the roughness of the surroundings was geometrically modeled instead of applying a roughness length. For the first approach, the domain was divided into two main areas: close to the buildings and at a distance from the buildings (areas 2-4 and area 1 in Figure 2, respectively). Close to the buildings, the roughness length of the ground boundary was set to a constant $z_0 = 0.03$ m while the values of z_0 in the outer region were varied. For applying z_0 to ANSYS Fluent, the sand-grain roughness k_s [m] had to be calculated using following equation (Blocken, 2015):

$$k_s = \frac{9.973\ z_0}{C_s} \tag{10}$$

$C_s = 1.0$ [-] is the roughness constant.

For the second approach, namely the geometrical modeling of roughness, the surroundings were modeled according to the descriptions of the investigated classes provided by Wieringa (1992). Classes 4, 5, and 6 were modeled as low hedges, vineyards & shelterbelts, and agricultural environment, respectively. For class 7, the actual surroundings of the university building were modelled (Figure 5). The domain was upsized to L = 798 m, creating a space of 180 m up and downwind of the buildings for the modeling of surroundings. $z_{0,ground} = 0.03$ m was imposed to the ground around the buildings and the surroundings. In the outer area close to the in- and outlet where no geometrical surroundings were created. Instead, the corresponding roughness value was applied to the ground.

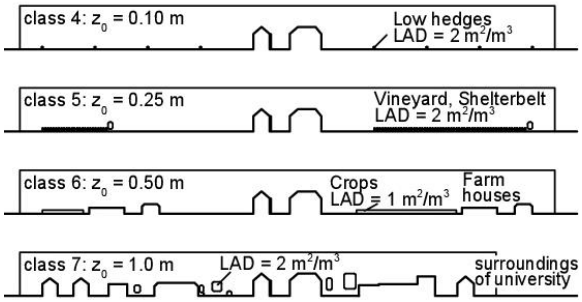

Figure 5: Geometrical modeling of roughness in the extended medium-mesh zone (area 2 in Figure 2)

Results and discussion

Figure 6 compares the course of air velocities at the bare façade and the greened façade in relation to the distance from the wall. At the bare façade, velocity rises quickly to around 0.40 m/s at the first floor level and 0.75 m/s at the second floor level. Completely different patterns were observed on the greened façade. In general, the variation in velocity within the regions between the components of the LWS is remarkably smaller on the first floor level compared to the second floor level. The velocity increases within the LWS until reaching a maximum of 0.15 m/s at the first floor level and 0.65 m/s at the second floor height. Subsequently, the velocity strongly drops due to the shear stress behind the PV module. In front of the PV modules, velocities reach values of those at the bare façade, but at a higher distance from the wall.

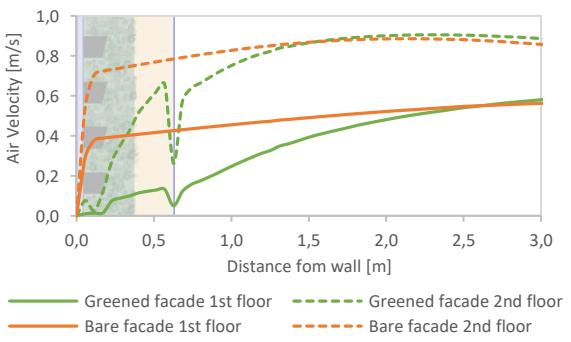

Figure 6: Air velocity in front of the investigated wall with and without the LWS at the first and second floor levels (in the style of Perini et al. (2011))

Figure 7 shows the results of velocities and air change rates of roughness length simulations compared with the results of geometrically modeled roughness. Overall, with increasing roughness length, the velocity rises at second floor height and slightly decreases at first floor height except for the air gap behind the LWS, where the velocity increases. Velocities derived from simulations of the geometrically modeled roughness show similar behavior and similar magnitudes compared to results from the roughness length. On the first floor, results are slightly lower for the geometrical roughness in comparison with results from roughness length. The opposite occurs only for roughness class 7 in the area behind PV. Comparing the deviations of results from geometrical roughness and roughness length, results for class 4 show lowest relative deviation with 20% on average. The highest average relative deviation occurs with 50% at roughness class 5. Observing the different regions of the LWS, the lowest deviation occurs within the air gap behind the LWS. Comparing results from first and second floor height, the behavior at the second floor height is opposite. Here, the magnitude of velocity resulting from geometrical roughness is higher compared to velocities derived from simulations with roughness length. At this height, lowest relative deviations for the second floor can be found in the area behind PV for all classes. For class 6, it is as low as 12%. In general, results at the first floor differ less than at second floor height. The values of ACH vary between 250 h^{-1} and 1350 h^{-1} within the air gap behind the LWS, 400 h^{-1} and 1000 h^{-1} within the foliage, and 1200 h^{-1} to 2150 h^{-1} in the area behind PV. A comparison of the distribution of velocity within the greening module from roughness length and geometrically modeled roughness is given in Figure 8 for z_0 = 0.10 m and z_0 = 1.0 m. Color maps underline the statement that for geometrical roughness, velocities on the second floor are higher than for roughness length. On the first floor, velocities are lower in the case of the geometrical roughness except in the air gap behind the PV module for z_0 = 1.0 m.

Generally speaking, values of air velocities derived in this study are similar to those mentioned in literature. E.g., Perini et al. (2011) provide experimental data of an LWS among others located in a rural area. They reported average air velocities of 0.41 m/s within the foliage and 0.10 m/s within a 4-cm air gap behind the LWS. In the present study, air velocities vary around 0.10 m/s to 0.20 m/s within this air gap. Within the foliage, the velocity resulted to around 0.40 m/s. However, the measuring time of the reviewed study was only around 30 minutes and the living wall system was not equipped with a PV module. Rahiminejad and Khovalyg (2021) give an overview of air velocities and ACH reported by numerous studies for different claddings of a façade with air cavities of 2 cm to 5 cm. They mention air velocities of 0.15 m/s within a cavity behind a steel plate, and 0.195 m/s behind vertical rain screen battens. They also give ACH derived from CFD simulations, e.g. in a range of less than 200 h^{-1} to almost 900 h^{-1} for a cavity of 5 cm. However, the comparison of ACH is not straightforward, as they are calculated in dependency on the height of the air cavity, which might be different in the present study. Other influences on the results could be the different areas the studies were located at. This applies to the surroundings of the area as well. Also, the weather and climate conditions and the orientation of wind flow can be severely influential on the results.

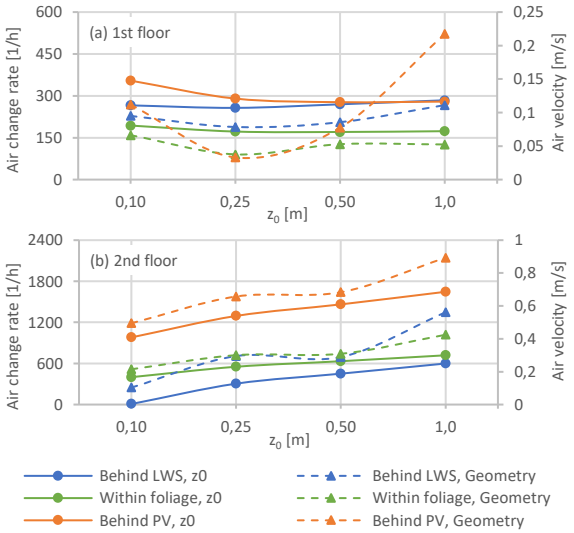

Figure 7: Average air velocities and air change rates from the different simulated models at the first floor (a) and second floor levels (b)

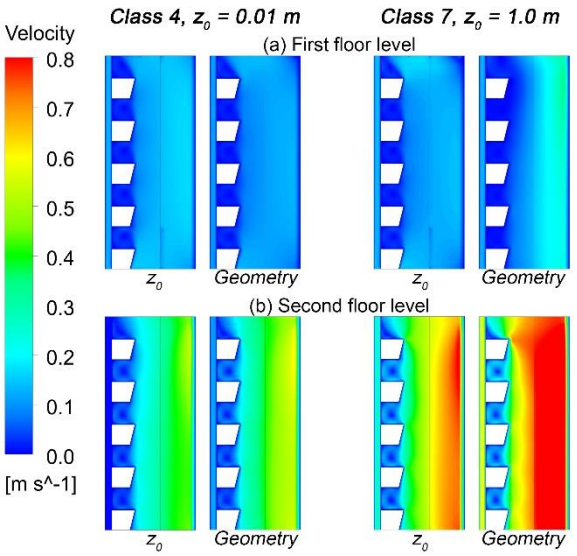

Figure 8: Color maps of velocity within the façade greening modules at the first floor (bottom) and second floor (top)

Conclusions

In the present study, the impact on airflow by a façade greening system was studied by means of CFD

simulations using ANSYS Fluent with different roughness of the surroundings. After generating the domain, the vegetation model was validated with measurement data, and the realizable k-ε model was chosen. The grid and convergence criteria were chosen based on sensitivity analyses. Overall, CFD results showed reduced air velocities within the LWS in comparison to a bare façade. Velocities were lowest within the air gap behind the LWS, rarely exceeding 0.15 m/s. Within the foliage, velocities increased to around 0.20 m/s, in some cases higher. The highest velocities were found behind the PV module at around 0.50 m/s on average. This provides air change rates of 360 h^{-1}, 480 h^{-1}, and 1200 h^{-1} for the different areas, respectively. The results indicated that CFD simulations with different roughness characteristics of the surroundings resulted in different trends for the LWS at the two investigated heights. In general, air velocities increased with increasing roughness at the second floor level. This was the case for both the modeling of the roughness length z_0 as well as the roughness geometry, which yielded results of similar magnitude. The first floor level, on the other hand, showed lower changes in velocity as the roughness increased.

Acknowledgement

This study was conducted as part of the research project VertiKKA: Vertikale Klimakläranlage zur Steigerung der Ressourceneffizienz und Lebensqualität in urbanen Räumen (vertikka.de) funded by the German Federal Ministry of Education and Research (BMBF), Grant No. 033W108G. Their support is highly cherished. Also, special thanks to Morteza Mosayebzadeh for his massive support.

References

Alsaad, H., Hartmann, M., Hilbel, R., Voelker, C., 2022a. ENVI-met validation data accompanied with simulation data of the impact of facade greening on the urban microclimate. Data in Brief 42, 108200.

Alsaad, H., Hartmann, M., Hilbel, R., Voelker, C., 2022b. The potential of facade greening in mitigating the effects of heatwaves in Central European cities. Building and Environment 216, 109021.

Alsaad, H., Hartmann, M., Voelker, C., 2022c. Hygrothermal simulation data of a living wall system for decentralized greywater treatment. Data in Brief 40, 107741.

Alsaad, H., Hartmann, M., Voelker, C., 2022d. The effect of a living wall system designated for greywater treatment on the hygrothermal performance of the facade. Energy and Buildings 255, 111711.

Alsaad, H., Voelker, C., 2021. Heat and moisture transport through a living wall system designated for greywater treatment. Proceedings of BS2021: 17th Conference of the International Building Performance Simulation Association, Belgium.

Amiro, B.D., 1990. Comparison of turbulence statistics within three boreal forest canopies. Boundary-Layer Meteorol 51 (1-2), 99–121.

Blocken, B., 2015. Computational Fluid Dynamics for urban physics: Importance, scales, possibilities, limitations and ten tips and tricks towards accurate and reliable simulations. Building and Environment 91, 219–245.

Franke, J., Hellsten, A., Schlünzen, H., Carissimo, B. (Eds.), 2007. Best parctice guideline for the CFD simulation of flows in the urban environment: COST Action 732.

Gromke, C., Blocken, B., 2015. Influence of avenue-trees on air quality at the urban neighborhood scale. Part I: quality assurance studies and turbulent Schmidt number analysis for RANS CFD simulations. Environmental pollution 196, 214–223.

Gromke, C., Blocken, B., Janssen, W., Merema, B., van Hooff, T., Timmermans, H., 2015. CFD analysis of transpirational cooling by vegetation: Case study for specific meteorological conditions during a heat wave in Arnhem, Netherlands. Building and Environment 83, 11–26.

Perini, K., Ottelé, M., Fraaij, A., Haas, E.M., Raiteri, R., 2011. Vertical greening systems and the effect on air flow and temperature on the building envelope. Building and Environment 46 (11), 2287–2294.

Rahiminejad, M., Khovalyg, D., 2021. Review on ventilation rates in the ventilated air-spaces behind common wall assemblies with external cladding. Building and Environment 190, 107538.

Richards, P., Hoxey, R., 1993. Appropriate boundary conditions for computational wind engineering models using the k-ϵ turbulence model. Journal of Wind Engineering and Industrial Aerodynamics 46-47, 145–153.

Susorova, I., Azimi, P., Stephens, B., 2014. The effects of climbing vegetation on the local microclimate, thermal performance, and air infiltration of four building facade orientations. Building and Environment 76, 113–124.

Tominaga, Y., Mochida, A., Yoshie, R., Kataoka, H., Nozu, T., Yoshikawa, M., Shirasawa, T., 2008. AIJ guidelines for practical applications of CFD to pedestrian wind environment around buildings. Journal of Wind Engineering and Industrial Aerodynamics 96 (10-11), 1749–1761.

Wieringa, J., 1992. Updating the Davenport roughness classification. Journal of Wind Engineering and Industrial Aerodynamics 41 (1-3), 357–368.